

“©2020 IEEE. Personal use of this material is permitted. Permission from IEEE must be obtained for all other uses, in any current or future media, including reprinting/republishing this material for advertising or promotional purposes, creating new collective works, for resale or redistribution to servers or lists, or reuse of any copyrighted component of this work in other works.”

# Communication

## Synthesis of Multibeam Sparse Circular-Arc Antenna Arrays Employing Refined Extended Alternating Convex Optimization

Yanhui Liu, *Senior Member, IEEE*, Yuqi Yang, Pan Wu, Xinyu Ma, Ming Li, Kai-Da Xu, *Senior Member, IEEE*, and Y. Jay Guo, *Fellow, IEEE*

**Abstract**—A refined extended alternating convex optimization (REACO) method is presented to synthesize multibeam sparse circular-arc antenna arrays with minimum element spacing control by considering real antenna array structure characteristics. This method consists of initial step and a few refining steps. At the initial step, an initial array with dense elements distributed on a circular-arc is considered, and its array manifold vector is described by rotating a simulated isolated element pattern (IEP) without considering element mutual coupling. The collective excitation coefficient vector (CECV) and its energy bound are introduced for each element, and consequently the common element positions for generating desired multibeam patterns can be found by minimizing the number of active CECVs under multiple constraints. This minimization problem is further formulated as performing a sequence of alternating convex optimization (ACO) in which the CECV and an auxiliary weighting vector are alternately chosen as the optimization variables, so that the minimum element spacing constraint can be easily dealt with. Once the initial optimization step is finished, a few refining steps are performed in which the element positions and excitations are successively updated in each step by renewing the array manifold vector through rotating the simulated nearby active element patterns (AEPs) of the antenna array obtained at the previous step. In such a way, the mutual coupling can be incorporated into the multibeam sparse array synthesis. An example of synthesizing a sparse circular-arc conformal array with 23 beams covering the space from  $-63.25^\circ$  to  $63.25^\circ$  is conducted to validate the effectiveness and advantage of the proposed method.

**Index Terms**—Sparse circular-arc array, alternating convex optimization, multibeam pattern synthesis, minimum element spacing control

### I. INTRODUCTION

**S**INGLE beam antenna arrays usually provide either a directive beam with high gain radiation for a limited spatial coverage, or a shaped beam with limited gain over a predefined angular range. In contrast, multibeam antenna arrays which can generate a number of independent high-gain directive beams across a wide spatial range are more promising in many applications such as multi-user mobile communications and multi-target detection systems [1], [2]. Especially, when we consider a multibeam circular-arc antenna array whose elements are placed along a circle or conforming with a cylinder, the generated multiple beams can cover a much larger angular range with less gain loss than that obtained by a linear array [3], [4]. However, the multibeam antenna array requires implementation of multiple excitation distributions in either radio-frequency (RF) or digital domain, which significantly increases the cost of the whole

system. In this situation, reducing the number of elements in the multibeam antenna array is of great importance for some applications where the weight and the cost of the system are limited [5].

As is well known, using nonuniform spacing with optimized positions provides possibility for a sparse array solution. In the past, many advanced methods for synthesizing nonuniformly spaced arrays have been developed. They mainly include analytical techniques [6], [7], stochastic optimization algorithms [8], [9], compressive sensing (CS) and Bayesian CS techniques [10]–[12], matrix pencil methods (MPM) [13]–[15], the reweighted  $\ell_1$ -norm optimization techniques [16]–[18] and the efficient inflating-deflating exploration algorithm (IDEA) [19]. Among them, a majority of methods deal with position selection or optimization for linear or planar arrays with assumed isotropic elements, and they cannot be directly applied to circular-arc antenna arrays in which all the elements face in different directions and the element patterns vary with their positions on the arc. Few methods presented in [6], [9] and [12], can optimize the element positions on a circular or cylindrical surface but they still adopt isotropic element assumption or simple analytical expressions to describe element patterns. Although this can greatly simplify the synthesis problem, it results in limited applications as some significant factors including the antenna element structure, mutual coupling and platform effect in the practical circular-arc array are not considered. Besides, most of these techniques are developed to synthesize a single pattern. When applied to a multibeam case, they may obtain different position results for different beams.

Recently, some advanced techniques have been developed to incorporate the mutual coupling into the element position synthesis [20]–[23]. In [20], element positions are iteratively updated by finding the optimal position perturbations using convex optimization and mutual coupling is included by employing fast full-wave simulation scheme to obtain active element patterns (AEPs) at each iteration. In [21], the mutual coupling is successfully included in the element position selection by incorporating phase-shifted AEPs into the iterative reweighted  $\ell_1$ -norm optimization. More recently, these techniques have been extended to effectively deal with multibeam synthesis for sparse linear and planar arrays [22], [23]. However, to the best of our knowledge, element position optimization including mutual coupling for conformal arrays have not yet been reported.

Another issue to be addressed is the minimum element spacing control which is essential for synthesizing practical nonuniformly spaced antenna arrays. The challenge is that this constraint is highly nonlinear. Some stochastic optimization algorithms such as the improved particle swarm optimization (IPSO) adopted in [27] may be capable of finding the globally optimal solution, but they are in general time consuming. More efficient sparse array synthesis techniques such as the CS-based synthesis methods, the reweighted  $\ell_1$ -norm optimization methods and the MPM cannot directly deal with this constraint even in the case of linear or planar arrays. Consequently, some of the synthesized element positions may be spaced too closely to be realized in practice. To overcome this problem, several

Manuscript received March 9, 2019; revised October 19, 2019. This work was supported in part by the National Natural Science Foundation of China (NSFC) under Grant No. 61871338, and in part by the University of Technology Sydney. (Corresponding author: Yanhui Liu).

Y. Liu is with the School of Electronic Science and Engineering, University of Electronic Science and Technology of China, Chengdu 611731, China (email: yhliu@uestc.edu.cn).

Y. Yang, P. Wu, and X. Ma are with Institute of Electromagnetics and Acoustics, Xiamen University, Fujian 361005, China.

K.-D. Xu is with the School of Information and Communications Engineering, Xi'an Jiaotong University, Xi'an 710049, China.

M. Li and Y. Jay Guo are with the Global Big Data Technologies Centre, University of Technology Sydney (UTS), NSW 2007, Australia.

merging techniques have been presented to post-process the results obtained from the CS technique or the reweighted  $\ell_1$ -norm optimization methods [12], [24]–[26], and the closely spaced positions are merged to meet the minimum element spacing constraint. Despite its effectiveness, such post-processing may result in deterioration in the pattern performance. In [28], a non-super directivity matrix is introduced into the reweighted  $\ell_1$ -norm optimization to control the minimum element spacing for planar array layout optimization. Recently, an iterative constrained convex optimization technique is presented to synthesize space-tapered multibeam linear arrays where the element position distributions are successively updated under a preset minimum element spacing constraint [29].

Recently, we presented an alternating convex optimization (ACO) method in which the sparse array synthesis problem is formulated as a sequence of alternating weighted  $\ell_1$ -norm optimizations [30]. Different from the original reweighted  $\ell_1$ -norm optimization method, the ACO method alternately chooses the element excitation vector and weighting vector as the optimization variables, so that the minimum element spacing constraint can be easily incorporated into the optimization process. However, the ACO method in [30] was presented to synthesize single-beam sparse linear arrays with the isotropic element assumption. In this work, we will present a refined extended ACO (REACO) method to synthesize multibeam sparse circular-arc arrays with minimum element spacing control by considering mutual coupling as well as platform effect. The proposed REACO method differs from the original ACO as follows: a) for the multibeam sparse circular-arc array, each element is associated with multiple excitation weights for different beam patterns. In this situation, a collective excitation coefficient vector (CECV) and its energy bound are introduced for each element. Then the ACO is extended to minimize the number of active CECVs with the minimum element spacing constraint so as to find the common element positions on the circular-arc for multibeam requirements. This is much different from direct minimization of the number of excitations used in the original ACO for the single-beam sparse linear array synthesis; b) the REACO method deals with a more complicated array model by considering circular-arc antenna array structure including mutual coupling and platform effect. Inspired by the works in [20]–[23], the REACO method at first performs an initial optimization step without considering mutual coupling to find a rough distribution of element positions and then takes a few refining steps to successively update the element positions and excitations by using the simulated nearby active element patterns (AEPs) of the antenna array obtained at the previous step. In this way, the mutual coupling can be incorporated into the refining steps. An example of synthesizing a sparse circular-arc conformal antenna array having 23 beams covering the space from  $-63.25^\circ$  to  $63.25^\circ$  is conducted to validate the effectiveness of the proposed method.

## II. MULTIBEAM SPARSE CIRCULAR-ARC ARRAY SYNTHESIS

### A. Multibeam Circular-arc Array Model

To synthesize a multibeam sparse circular-arc antenna array, we can first define a densely spaced array located on a circular arc, and then select the best element positions from them with optimized multiple sets of excitations, each set of excitations being associated with one desired beam. Let us consider a circular-arc array with  $N$  potential elements which are located at the angles  $\{\phi_1, \phi_2, \dots, \phi_N\}$  on a circle with radius of  $R$  in  $xy$ -plane. For simplicity, we assume that the potential elements are equally spaced with  $\phi_n = \phi_0 + n\Delta_\phi$  for  $n = 1, 2, \dots, N$  where the element spacing should satisfy  $2R \sin(\Delta_\phi/2) \ll \lambda$  for a dense potential position distribution. We further assume that this array radiates  $M$  overlapping beams,

and each beam corresponds to a set of excitations. Then, the  $m$ th ( $m = 1, 2, \dots, M$ ) array pattern at  $xy$ -plane is given by

$$F^{(m)}(\varphi) = \sum_{n=1}^N w_n^{(m)} a_n(\varphi) e^{-j\beta R \cos(\varphi - \phi_n)} \quad (1)$$

where  $j = \sqrt{-1}$ ,  $\beta = 2\pi/\lambda$  is the wavenumber in free space, and  $w_n^{(m)}$  denotes the complex excitation of the  $n$ th element for the  $m$ th array pattern.  $\phi_n$  is the angle of the circle at which the  $n$ th element is located, and  $a_n(\varphi)$  is the pattern of the  $n$ th element. The array pattern can be rewritten as the following form

$$F^{(m)}(\varphi) = \mathbf{a}^T(\varphi) \mathbf{w}^{(m)} \quad (2)$$

where

$$\mathbf{a}(\varphi) = \begin{bmatrix} a_1(\varphi) e^{-j\beta R \cos(\varphi - \phi_1)} \\ a_2(\varphi) e^{-j\beta R \cos(\varphi - \phi_2)} \\ \vdots \\ a_N(\varphi) e^{-j\beta R \cos(\varphi - \phi_N)} \end{bmatrix} \quad (3)$$

$$\mathbf{w}^{(m)} = [w_1^{(m)}, w_2^{(m)}, \dots, w_N^{(m)}]^T \quad (4)$$

In the above, the superscript ' $T$ ' denotes the transpose of a matrix, and  $\mathbf{a}(\varphi)$  is called the array manifold vector.

Note that in practical application, a circular-arc antenna array usually conforms with a cylindrical platform, so that its antenna elements would face in different directions and the element pattern  $a_n(\varphi)$  varies with its position on the platform. If mutual coupling is ignored or weak enough, the element patterns among different elements have the rotationally invariant property given by

$$a_n(\varphi) \approx a_p(\varphi - (\phi_n - \phi_p)) \quad (5)$$

This relationship will be adopted to approximately construct the array manifold vector for sparse array optimization.

### B. Multibeam Sparse Circular-arc Array Synthesis Problem

The problem of synthesizing a sparse circular-arc array with multiple overlapping beams under minimum element spacing control can be formulated as that of minimizing the number of elements under multiple different constraints. For each of beam patterns, multiple constraints can be used to accurately control the maximum beam direction and sidelobe level (SLL). They are given as follows:

i) *Multibeam direction constraints:*

$$\mathbf{a}^T(\varphi) \mathbf{w}^{(m)} = 1, \quad \text{for } \varphi = \varphi_{\text{look}}^{(m)} \quad (6)$$

To avoid the  $m$ th beam direction deviating from the desired one, a derivative constraint of  $\partial |\mathbf{a}^T(\varphi) \mathbf{w}^{(m)}|^2 / \partial \varphi = 0$  at  $\varphi = \varphi_{\text{look}}^{(m)}$  can be used. By combining that  $\mathbf{a}^T(\varphi_{\text{look}}^{(m)}) \mathbf{w}^{(m)} = 1$ , the derivative constraint can be further simplified as the following

$$\frac{\partial \{ \text{Re}[\mathbf{a}^T(\varphi) \mathbf{w}^{(m)}] \}}{\partial \varphi} = 0, \quad \text{for } \varphi = \varphi_{\text{look}}^{(m)} \quad (7)$$

ii) *Sidelobe constraint for each beam:*

$$|\mathbf{a}^T(\varphi) \mathbf{w}^{(m)}|^2 \leq U_{\text{SL}}^{(m)}, \quad \text{for } \varphi \in \Psi_{\text{SL}}^{(m)} \quad (8)$$

where  $\Psi_{\text{SL}}^{(m)}$  and  $U_{\text{SL}}^{(m)}$  are the angle range and the specified upper bound of the sidelobe for the  $m$ th beam, respectively. Usually,  $U_{\text{SL}}^{(m)}$  can be set as the same for different beam patterns. That is,  $U_{\text{SL}}^{(m)} = U_{\text{SL}}$  for  $m = 1, 2, \dots, M$ .

Clearly, if the element positions of an array are fixed, the problem with above constraints can be solved by using convex optimization [31]. However, the considered problem is to reduce the number of elements by selecting the common element positions for multiple

beam patterns. It means that a large number of element positions must be discarded from the initial dense distribution. Since each antenna element in the multibeam circular-arc array is associated with multiple excitations (implemented in either RF or digital multibeamforming network), one element can be discarded only if all the excitations related to this element are simultaneously minimized to zeros. This is different from single-beam sparse array synthesis case. To overcome this problem, we introduce a collective excitation coefficient vector (CECV) which is given by

$$\check{\mathbf{w}}_n = \{w_n^{(1)}, w_n^{(2)}, \dots, w_n^{(M)}\}^T. \quad (9)$$

By introducing an auxiliary variable  $t_n$ , we can constrain the energy bound of each  $\check{\mathbf{w}}_n$  ( $n = 1, 2, \dots, N$ ) as the following

$$t_n \geq \left\| w_n^{(1)}, w_n^{(2)}, \dots, w_n^{(M)} \right\|_2. \quad (10)$$

Then, the problem of reducing the number of selected elements is equivalent to minimizing the  $\ell_0$ -norm  $\|\mathbf{t}\|_0$  under the constraints of (6)-(8) and (10), where  $\mathbf{t} = [t_1, t_2, \dots, t_N]^T$ .

Another problem concerned is the minimum element spacing constraint that is used to avoid the presence of some closely spaced element positions in the synthesized result. In the case of circular-arc arrays, this constraint can be given by

$$d \geq d_{\min} = 2R \sin\left(\frac{Q\Delta\phi}{2}\right) \quad (11)$$

where  $d$  is the spacing between arbitrary two selected elements,  $d_{\min}$  is the required minimum element spacing, and  $Q = \lceil 2 \arcsin(d_{\min}/2R) \rceil / \Delta\phi$  is the total number of potential positions contained within the required minimum spacing. This means there are at the least  $(Q - 1)$  unselected potential positions between the selected elements. By integrating all the constraints, we can formulate the whole synthesis problem as the following

$$\begin{cases} \min_{\{w_n^{(m)}, t_n; \substack{m=1, \dots, M \\ n=1, \dots, N}\}} \|\mathbf{t}\|_0 \\ \text{Const.} \begin{cases} t_n \geq \left\| w_n^{(1)}, w_n^{(2)}, \dots, w_n^{(M)} \right\|_2, & (a) \\ \mathbf{a}^T(\varphi) \mathbf{w}^{(m)} = 1 \text{ and } \frac{\partial \{\text{Re}[\mathbf{a}^T(\varphi) \mathbf{w}^{(m)}]\}}{\partial \varphi} = 0, & (b) \\ \text{for } \varphi = \varphi_{\text{look}}^{(m)} \quad (m = 1, 2, \dots, M); \\ |\mathbf{a}^T(\varphi) \mathbf{w}^{(m)}|^2 \leq U_{\text{SL}}^{(m)}, \text{ for } \varphi \in \Psi_{\text{SL}}^{(m)} & (c) \\ (m = 1, 2, \dots, M); \\ d \geq 2R \sin(Q\Delta\phi/2), \text{ } d \text{ is the distance between} & (d) \\ \text{arbitrary two selected elements } (t_n \neq 0). \end{cases} \end{cases} \quad (12)$$

### C. Refined Extended Alternating Convex Optimization Method

The problem in (12) is a NP-hard combinatorial optimization problem due to the  $\ell_0$ -norm optimization objective function. The reweighted  $\ell_1$ -norm optimization technique is an alternative way to efficiently produce a sparse solution, and the technique has been applied to many single-beam sparse array synthesis problems. By virtue of introducing the CECV, the reweighted  $\ell_1$ -norm optimization technique presented in [16]- [18] can be extended to deal with the multibeam sparse circular-arc array synthesis problem. That is,

$$\begin{cases} \min_{\{w_n^{(m)}, t_n; \substack{m=1, \dots, M \\ n=1, \dots, N}\}} \mathbf{g}^T \mathbf{t} \\ \text{under Const. 12(a)-(c)} \end{cases} \quad (13)$$

where  $\mathbf{g} = [g_1, g_2, \dots, g_N]^T$  is a weighting vector. In the reweighted  $\ell_1$ -norm optimization technique,  $g_n$  is usually set as  $g_n = 1/(t_n + \delta)$  where  $\delta$  is a small positive number, and it can be successively

updated by adopting new  $t_n$  at each iteration. This technique can be called the extended reweighted  $\ell_1$ -norm optimization technique. It does produce a multibeam sparse circular-arc array solution, but the minimum element spacing constraint cannot be easily incorporated into the synthesis process.

In [30], we presented an ACO method to synthesize single-beam sparse linear array with the minimum element spacing control. In the ACO method, the excitation vector and the weighting vector are alternatively chosen as the optimization variables, and  $\mathbf{g}$  is updated by solving a convex optimization problem at each iteration. In this situation, the minimum element spacing constraint can be transformed as controlling the distribution of elements in  $\mathbf{g}$  by using a sequence of additional constraints. This idea can be further extended to control the minimum element spacing for the multibeam sparse circular-arc array synthesis as follows

$$\begin{cases} \min_{\{w_n^{(m)}, t_n; \substack{m=1, \dots, M \\ n=1, \dots, N}\}} \mathbf{g}^T \mathbf{t} \\ \text{under Const. 12(a)-(c)} \end{cases} \quad (14a)$$

$$\begin{cases} \min_{\mathbf{g}} \mathbf{g}^T |\mathbf{t}_*| \\ \text{Const.} \begin{cases} 0 \leq \mathbf{g} \leq 1; \\ \mathbf{1}^T \mathbf{g}(n : n + Q - 1) \geq Q - 1 \\ \text{(for } n = 1, \dots, N - Q + 1). \end{cases} \end{cases} \quad (14b)$$

In Problem (14a),  $w_n^{(m)}$  ( $m = 1, \dots, M$ ,  $n = 1, \dots, N$ ) and  $\mathbf{t}$  are optimization variables under a given  $\mathbf{g}_*$  which is obtained by solving Problem (14b) at the previous step, and in Problem (14b),  $\mathbf{g}$  is the optimization variable under a given  $\mathbf{t}_*$  that is just obtained from (14a). In the initial iteration,  $\mathbf{g}_*$  can be chosen as random numbers or just set as  $\mathbf{g}_* = 1$ . The two subproblems are weighted  $\ell_1$ -norm minimization problems, and they can alternatively solved by using convex optimization. Now, let us consider the solution to Problem (14b). It is obvious that each  $Q$ -length segment  $\mathbf{g}(n : n + Q - 1)$  (for  $n = 1, \dots, N - Q + 1$ ) of the solution obtained from Problem (14b) will have at the least  $Q - 1$  entries of '1' and at the most one entry of '0', provided that there are no two identical elements in the same segment of  $\mathbf{t}_*$ . Thus, in each iteration, the entries of '1' in  $\mathbf{g}_*$  will heavily penalize the corresponding energy bound of the collective excitation coefficient vector in  $\mathbf{t}$  for Problem (14a), while the collective excitation coefficients with their energy bound in  $\mathbf{t}$  corresponding to '0' entries of  $\mathbf{g}_*$  will be remained. Since every  $Q$ -length segment of  $\mathbf{g}_*$  has at the most one entry of '0', no more than one corresponding element in each segment of  $\mathbf{t}$  will be remained and all others in this segment will be penalized to zeros. This explains how the extended ACO method works for controlling the minimum element spacing in the multibeam sparse circular-arc array synthesis.

Now, the remaining problem is that the element mutual coupling depends on the selected element positions, and thus the accurate array manifold vector  $\mathbf{a}(\varphi)$  is actually unknown before the element positions are determined. To deal with this problem, a refined extended ACO method (REACO) is presented. At the initial step, the mutual coupling is not considered in the synthesis. An isolated element pattern (IEP) is obtained by full-wave simulation of a single antenna element located at  $\phi = 0$  of a cylinder platform, and then the array manifold vector  $\mathbf{a}(\varphi)$  can be constructed by using the relationship  $a_n(\varphi) \approx a^{\text{IEP}}(\varphi - \phi_n)$  according to (5). Then the method finds the initial element positions and excitations by performing the extended ACO. Assume that  $P$  element positions with the angles of  $\Phi_s = \{\phi_{s1}, \phi_2, \dots, \phi_{sP}\} \subset \{\phi_1, \phi_2, \dots, \phi_N\}$  are selected. It should be noted that the synthesized multibeam patterns in this step may deviate very much from the real ones including mutual coupling. Thus, the REACO method takes a few more refining steps to include the mutual coupling effect into the multibeam sparse circular-arc

array synthesis. At the  $k$ th ( $k \geq 1$ ) refining step, full-wave simulation of the antenna array with the element positions obtained at the previous step is performed, and then the simulated active element patterns (AEPs) are used to approximate the element patterns of  $\mathbf{a}(\varphi)$  at their nearby potential positions. That is given by

$$a_n(\varphi) \approx a_{sp}^{\text{AEP}}(\varphi - (\phi_n - \phi_{sp}^{(k-1)})) \quad (15)$$

where  $p = \min\{|\phi_n - \phi_{sp}^{(k-1)}|; \phi_{sp}^{(k-1)} \in \Phi_s^{(k-1)}\}$ , and  $a_{sp}^{\text{AEP}}(\varphi)$  is the AEP of the antenna element nearest to the potential position  $\phi_n$ . Once  $\mathbf{a}(\varphi)$  is renewed, one more refining optimization can be performed. To guarantee that the selected element positions are really close to those obtained at the previous step for accurate approximation of (15), we can add some additional constraints for controlling the distribution of  $\mathbf{g}$  when solving the problem (14b). That is, setting  $g_n = 1$  when  $R|\phi_n - \phi_{sp}^{(k-1)}| \geq 0.1\lambda$  for all  $\phi_{sp}^{(k-1)} \in \Phi_s^{(k-1)}$ . The refining optimization can be iteratively performed until the obtained element positions remaining the same. In general, few refining steps are required for the convergence. It should be noted that when the obtained element positions remain the same as those obtained at the previous step, the synthesized multi-beam patterns will be equal to the real ones including mutual coupling. This means that the obtained final multibeam patterns including mutual coupling have good performance since the synthesized ones are always obtained with multiple constraints on beam directions and sidelobe distributions. Note that the full-wave simulations used in the synthesis procedure can be accomplished by using either commercial softwares such as High Frequency Structure Simulator (HFSS) [32] or user-designed electromagnetic simulation codes. In the example given in the following, we use the HFSS tool to implement all the required full-wave simulations.

### III. NUMERICAL RESULTS

To verify the effectiveness of the proposed REACO method, we apply it to synthesize a multibeam sparse circular-arc conformal array with curved E-type patch antenna elements. The curved E-type patch antenna element mounted on a part of cylindrical surface is designed at the center frequency of 13 GHz, and its geometry is shown in Fig. 1. The size of the radiating E-type patch is about  $0.39\lambda$  at 13 GHz. The radius of the cylinder is chosen as  $R = 138.5$  mm which is about  $6\lambda$  at 13 GHz. Assume that the desired multibeam patterns have 23 beams with interval of  $5.5^\circ$  covering the space from  $-63.25^\circ$  to  $63.25^\circ$ , and each of beams has the first beamwidth (FNBW) of  $14^\circ$ . The desired SLL is set as  $U_{\text{SL}} = -16$  dB outside of the FNBW region for each beam pattern. At the initial step, we apply the proposed method without considering mutual coupling (i.e., the extended ACO) to find the element positions and multiple sets of excitations for the desired multibeam patterns. The initial array is set as a large number of potential element positions uniformly distributed within the angle range of  $-75^\circ$  to  $75^\circ$  on the cylinder surface. To check the effectiveness of the extended ACO for different potential element spacing settings, we choose the parameter  $\Delta_\phi = [0.9554^\circ, 0.4777^\circ, 0.2389^\circ]$  such that the potential element spacing  $d_0 = 2R \sin(\Delta_\phi/2) = [0.1, 0.05, 0.025]\lambda$ . Accordingly, the number of potential positions is  $N = [158, 315, 629]$ . Different minimum element spacing constraints between the selected elements are considered by adjusting the selection of  $Q$  and  $\Delta_\phi$  according to  $d_{\min} = 2R \sin(Q\Delta_\phi/2)$ , and they are set as  $d_{\min} = 0.5\lambda$  ( $Q = 5$ ) for the case of  $\Delta_\phi = 0.9554^\circ$ ,  $d_{\min} = [0.45, 0.5]\lambda$  ( $Q = [9, 10]$ ) for the case of  $\Delta_\phi = 0.4777^\circ$ , and  $d_{\min} = [0.45, 0.475, 0.5]\lambda$  ( $Q = [18, 19, 20]$ ) for the case of  $\Delta_\phi = 0.2389^\circ$ . In this step, the isolated element pattern (IEP) which is obtained by using HFSS simulation of a single element mounted on the cylinder is used

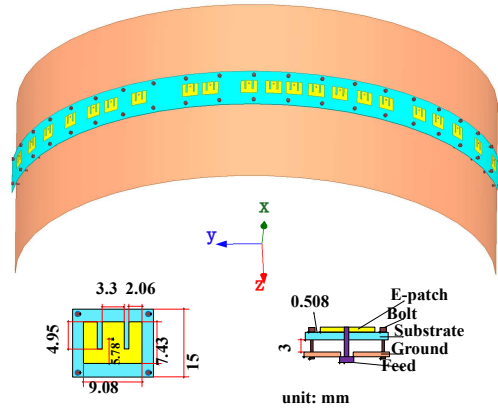


Fig. 1: Geometry of a 21-element circular-arc conformal array (with view of the E-type patch antenna on planar surface).

to construct the manifold vector  $\mathbf{a}(\varphi)$  without considering mutual coupling. Then the proposed method performs a series of alternating convex optimizations between Problem (14a) and (14b) for each test case. Besides, we also apply the extended reweighted  $\ell_1$ -norm optimization in (14) to synthesize the same example for comparison.

Table I lists the synthesis results of the proposed method at the initial step and the extended reweighted  $\ell_1$ -norm optimization in terms of the synthesized minimum and maximum element spacings, the number of selected elements as well as the maximum SLL (i.e., the maximum one for all the multibeam patterns). As can be seen, for all the test cases, both of the methods can obtain the multibeam pattern results satisfying the SLL requirement. For example, Fig. 2(a) shows the synthesized multibeam patterns by the proposed method at the initial step with  $\Delta_\phi = 0.4777^\circ$  and  $d_{\min} = 0.5\lambda$  ( $Q = 10$ ), and Fig. 2(b) shows the pattern result by the extended reweighted  $\ell_1$ -norm minimization with the same  $\Delta_\phi$ . It is confirmed that the obtained multibeam patterns by both of the methods do meet the  $-16$  dB SLL bound. However, the required number of elements for these two methods are slightly different. For the case of  $\Delta_\phi = 0.4777^\circ$  and  $0.2389^\circ$ , the synthesized arrays by the proposed method at the initial step have less elements. It is important that the arrays synthesized by the proposed method always meet the specified minimum element spacing constraints for all the test cases given in Table I. However, this is not true for the extended reweighted  $\ell_1$ -norm optimization where the minimum element spacing cannot be controlled and the obtained arrays generally cannot meet the required minimum spacing constraints in such a complicated multibeam synthesis situation. For example, for the case of  $\Delta_\phi = 0.4777^\circ$ , the obtained element position angles by the proposed method and the extended reweighted  $\ell_1$ -norm optimization are listed in Table II. The obtained minimum element spacing by the extended reweighted  $\ell_1$ -norm optimization is only  $0.35\lambda$  existing between the 10th and 11th elements. Such an array is unrealistic since the size of the E-type patch antenna element is  $0.39\lambda$ . This does not happen for the proposed method for all test cases.

All the above synthesis results based on the rotated IEP do not include the mutual coupling. The multibeam patterns for real antenna array structures may deviate much from the synthesized ones. For example, consider the synthesized 22-element array by the proposed method at the initial step with  $\Delta_\phi = 0.4777^\circ$  and  $d_{\min} = 0.5\lambda$ , and its element positions are given in the first column of Table II. Based on these positions, we can build the sparse cylindrical antenna array. Fig. 2(c) shows the obtained multibeam patterns including mutual coupling for the real antenna array structure through HFSS full-wave simulation with the same sets of excitations used in Fig. 2(a). As can be seen, the SLLs for the real multibeam patterns are all considerably

TABLE I: SYNTHESIS RESULTS WITHOUT CONSIDERING MUTUAL COUPLING BY THE PROPOSED METHOD AT THE INITIAL STEP AND THE EXTENDED REWEIGHTED  $\ell_1$ -NORM OPTIMIZATION TECHNIQUE ( $P$  IS THE NUMBER OF SELECTED ELEMENTS).

Initial array setting		Constrained $d_{\min}(\lambda)$	The proposed REACO					The extended reweighted $\ell_1$ -norm			
N	$\Delta_\phi$ ( $^\circ$ )		$Q$	Synth. spacings ( $\lambda$ )		$P$	SLL (dB)	Synth. spacings ( $\lambda$ )		$P$	SLL (dB)
			Min	Max			Min	Max			
158	0.9554	0.500	5	0.500	1.000	23	-16.00	0.400	1.500	22	-16.00
315	0.4777	0.450	9	0.450	1.000	22	-16.01	0.350	1.500	24	-16.00
		0.500	10	0.500	1.100	22	-16.03				
629	0.2389	0.450	18	0.450	1.725	22	-16.00	0.425	1.525	23	-16.00
		0.475	19	0.475	1.350	22	-16.00				
		0.500	20	0.500	1.350	22	-16.00				

TABLE II: THE SYNTHESIZED ELEMENT POSITION ANGLES ON THE CIRCULAR-ARC BY THE PROPOSED METHOD AT DIFFERENT STEPS AND THE EXTENDED REWEIGHTED  $\ell_1$ -NORM OPTIMIZATION ( $\Delta_\phi = 0.4777^\circ$ ,  $d_{\min} = 0.5\lambda$ ,  $R = 138.5$  MM).

Elem. Index	The REACO method				Reweighted $\ell_1$ -norm
	Initial	$k = 1$	$k = 2$	$k = 3$	
1	-74.522	-75	-75	-75	-75
2	-65.446	-64.968	-65.446	-64.968	-60.669
3	-55.892	-56.369	-55.892	-55.414	-49.204
4	-49.204	-49.204	-48.726	-48.248	-42.994
5	-42.516	-42.994	-42.516	-42.038	-39.172
6	-32.006	-32.484	-32.006	-32.484	-32.006
7	-26.274	-26.752	-26.752	-26.752	-24.841
8	-21.019	-21.019	-21.019	-20.541	-21.019
9	-14.809	-14.331	-14.331	-14.809	-14.809
10	-9.554	-9.076	-9.554	-9.554	-10.987
11	-4.777	-4.299	-4.299	-4.777	-7.166
12	0.478	0.478	0.478	0.955	-3.822
13	9.554	10.032	10.032	10.032	0
14	15.287	14.809	14.809	14.809	3.822
15	22.930	x	x	x	10.987
16	27.707	27.229	27.707	27.707	14.809
17	34.873	34.395	34.873	35.350	21.019
18	40.605	41.083	40.605	40.605	24.841
19	47.771	48.248	47.771	48.248	32.006
20	55.892	55.892	56.369	56.847	42.994
21	65.446	64.968	65.369	64.968	49.204
22	74.522	74.522	74.045	73.567	53.503
23					60.669
24					75

increased. For example, for the first left beam pattern, the SLL is increased from  $-16.01$  dB to  $-13.39$  dB, and its maximum beam direction is also changed from  $-60.5^\circ$  to  $-60.1^\circ$ . For the 18th beam pattern (counted from the first left beam), the SLL is increased from  $-17.36$  dB to  $-13.85$  dB, and its maximum beam direction is changed from  $33^\circ$  to  $32.5^\circ$ . The reason why the multibeam pattern performance degrades is that the AEPs for the real sparse antenna array deviates to some extent from those obtained by rotating the IEP which are assumed in the synthesis at the initial step. To improve the synthesis performance, the proposed method performs a few refining steps in which the array manifold vector is updated in each step by using the simulated AEPs of the antenna array obtained at the previous step. The element positions and excitations are successively refined. In this example, four refining steps are required to reach the convergence, and the element positions obtained at the 4th refining step remain the same as those at the 3rd refining step. Table II lists the obtained element positions at initial and first three refining steps. It is noted that the first refining step reduces the synthesized 22-element array at the initial step to only 21 elements. One element is saved by this refining step. The final synthesized multibeam patterns at the 4th refining step are equal to the real ones including mutual coupling since the selected element positions remain unchanged in this step. Thus, the final obtained real multibeam patterns have correct maximum beam directions and required SLL distributions as shown in Fig. 2(d). The obtained final excitations for 21 elements also vary from the excitations at the initial step for 22 elements. For example,

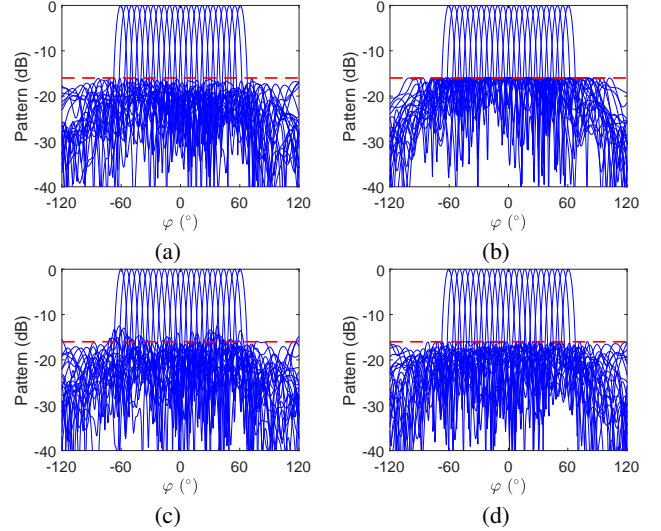


Fig. 2: The synthesized multibeam patterns without including mutual coupling (using rotated IEPs) by (a) the proposed REACO method at the initial step and (b) the extended reweighted  $\ell_1$ -norm optimization technique, as well as the simulated multibeam patterns including mutual coupling (using AEPs) by the proposed method (c) at the initial step and (d) with four refining steps.

Fig. 3(a) and (b) show the obtained excitation amplitudes and phases at the initial and 4th refining steps for the first left beam pattern, and Fig. 3(c) and (d) show the obtained results at the initial and 4th refining steps for the 18th beam pattern. In this example, we saved 36.4% elements if comparing with 33  $\lambda/2$ -spaced elements occupying the same circular-arc space from  $-75^\circ$  to  $75^\circ$ .

The time cost of the proposed method mainly comes from its refining steps. In each refining step of this example, on average the proposed method takes about 5.3 hours for the HFSS simulation of the obtained antenna array and 1.1 hours for the multibeam sparse array refining optimization, on a Dell workstation with Intel(R) Xeon(R) CPU E5-2697v4@2.30GHz. Besides, the proposed method at the initial step takes about 1.3 hours for initial sparse array synthesis without considering mutual coupling. The total time cost for the initial step and four refining steps is 26.9 hours in this example.

#### IV. CONCLUSION

We have presented a refined extended alternating convex optimization (REACO) method which can synthesize multibeam sparse circular-arc antenna arrays with minimum element spacing control, considering both mutual coupling and platform effect of a real antenna array structure. In this method, the collective excitation coefficient vector (CECV) and its energy bound are introduced for each potential element, and consequently the multibeam sparse circular-arc array synthesis problem is transformed as minimizing the number of active CECVs under multiple constraints. To deal with the minimum element spacing constraint, this minimization problem

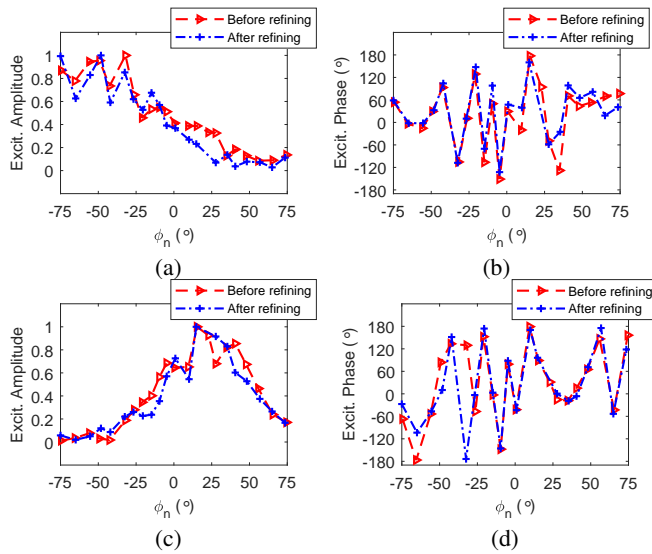


Fig. 3: The synthesized excitation distributions by the proposed method at the initial step and after four refining steps. (a) and (b) show the excitation amplitudes and phases for the first left beam pattern; (c) and (d) show the excitation amplitudes and phases for the 18th beam pattern.

is solved by means of alternating convex optimization (ACO) in which the weighting vector in each iteration is given by solving a sub-problem of constrained optimization other than simply setting in the reweighted  $\ell_1$ -norm optimization technique. In addition, the proposed method adopts a few refining steps to incorporate the mutual coupling into the multibeam sparse array synthesis. One example of synthesizing multibeam sparse circular-arc conformal arrays with E-shape microstrip antenna elements is conducted. Synthesis results show that the proposed method can control the minimum element spacing very well at all steps, and the final obtained sparse circular-arc array having 23 beams covering the space  $-63.25^\circ$  to  $63.25^\circ$ , saved 36.4% elements compared with the one with  $\lambda/2$ -spaced elements occupying the same arc. The obtained multibeam patterns including mutual coupling for real antenna array structure have correct beam directions and required sidelobe distributions.

## REFERENCES

- [1] W. Hong, *et al.*, "Multibeam antenna technologies for 5G wireless communications," *IEEE Trans. Antennas Propag.*, vol. 65, no. 12, pp. 6231-6249, Dec. 2017.
- [2] K.-B. Yu, "Digital beamforming of multiple simultaneous beams for improved target search," in *IEEE Radar Conference*, Pasadena, CA, USA, May 2009, pp. 4-8.
- [3] L. Josefsson and P. Persson, *Conformal Array Antenna Theory and Design*, Piscataway, NJ, USA: IEEE Press, 2006.
- [4] F. Ares, S. R. Rengarajan, J. A. F. Lence, A. Trastoy, and E. Moreno, "Synthesis of antenna patterns of circular arc arrays," *Electron. Lett.*, vol. 32, no. 20, pp. 1845-1846, Sep. 1996.
- [5] G. Toso, C. Mangenot, and A. G. Roederer, "Sparse and thinned arrays for multiple target search," in *Proc. 2nd EuCAP*, Edinburgh, U.K., Nov. 2007, vol. 16, pp. 1-4.
- [6] B. P. Kumar and G. R. Branner, "Generalized analytical technique for the synthesis of unequally spaced arrays with linear, planar, cylindrical or spherical geometry," *IEEE Trans. Antennas Propag.*, vol. 53, no. 2, pp. 621-634, Feb. 2005.
- [7] D. Caratelli and M. C. Viganó, "Analytical synthesis technique for linear uniform-amplitude sparse arrays," *Radio Sci.*, vol. 46, no. 4, Aug. 2011. doi:10.1029/2010RS004522.
- [8] R. L. Haupt, "Optimized element spacing for low sidelobe concentric ring arrays," *IEEE Trans. Antennas Propag.*, vol. 56, no. 1, pp. 266-268, Jan. 2008.
- [9] S. Liang, T. Feng, and G. Sun, "Sidelobe-level suppression for linear and circular antenna arrays via the cuckoo search-chicken swarm optimisation algorithm," *IET Microw. Antennas Propag.*, vol. 11, no. 2, pp. 209-218, Feb. 2017.
- [10] X. Zhao, Q. Yang, and Y. Zhang, "Compressed sensing approach for pattern synthesis of maximally sparse non-uniform linear array," *IET Microw. Antennas Propag.*, vol. 8, no. 5, pp. 301-307, Apr. 2014.
- [11] F. Viani, G. Oliveri, and A. Massa, "Compressive sensing pattern matching techniques for synthesizing planar sparse arrays," *IEEE Trans. Antennas Propag.*, vol. 61, no. 9, pp. 4577-4587, Sep. 2013.
- [12] G. Oliveri, E. T. Bekele, F. Robol, and A. Massa, "Sparsening conformal arrays through a versatile BCS-based method," *IEEE Trans. Antennas Propag.*, vol. 62, no. 4, pp. 1681-1689, Apr. 2014.
- [13] Y. Liu, Z. Nie, and Q. H. Liu, "Reducing the number of elements in a linear antenna array by the matrix pencil method," *IEEE Trans. Antennas Propag.*, vol. 56, no. 9, pp. 2955-2962, Sep. 2008.
- [14] Y. Liu, Q. H. Liu, and Z. Nie, "Reducing the number of elements in multiple-pattern linear arrays by the extended matrix pencil methods" *IEEE Trans. Antennas Propag.*, vol. 62, no. 2, pp. 652-660, Feb. 2014.
- [15] P. Gu, G. Wang, Z. Fan, and R. Chen, "Efficient unitary matrix pencil method for synthesizing wideband frequency patterns of sparse linear arrays" *IET Microw. Antennas Propag.*, vol. 12, no. 12, pp. 1871-1876, Sep. 2018.
- [16] S. E. Nai, W. Ser, Z. L. Yu, and H. Chen, "Beampattern synthesis for linear and planar arrays with antenna selection by convex optimization" *IEEE Trans. Antennas Propag.*, vol. 58, no. 12, pp. 3923-3930, Dec. 2010.
- [17] G. Prisco and M. D'Urso, "Maximally sparse arrays via sequential convex optimizations," *IEEE Antennas Wireless Propag. Lett.*, vol. 11, pp. 192-195, 2012.
- [18] B. Fuchs, "Synthesis of sparse arrays with focused or shaped beampattern via sequential convex optimizations," *IEEE Trans. Antennas Propag.*, vol. 60, no. 7, pp. 3499-3503, Jul. 2012.
- [19] D. Pinchera, M. D. Migliore, and G. Panariello, "Synthesis of large sparse arrays using IDEA (inflating-deflating exploration algorithm)," *IEEE Trans. Antennas Propag.*, vol. 66, no. 9, pp. 4658-4668, Sep. 2018.
- [20] B. Van Ha, S.N. Jha, C. Craeye, "Fast full-wave synthesis of printed antenna arrays including mutual coupling," *IEEE Trans. Antennas Propag.*, vol. 64, no. 12, pp. 5163-5171, Dec. 2016.
- [21] C. Bencivenni, M. V. Ivashina, R. Maaskant and J. Wettergren, "Design of maximally sparse antenna arrays in the presence of mutual coupling," *IEEE Antennas Wireless Propag. Lett.*, vol. 14, pp. 159-162, Sep. 2014.
- [22] C. Bencivenni, M. V. Ivashina, R. Maaskant and J. Wettergren, "Synthesis of maximally sparse arrays using compressive sensing and full-wave analysis for global earth coverage applications," *IEEE Trans. Antennas Propag.*, vol. 64, no. 11, pp. 4872-4877, Jul. 2016.
- [23] Y. Aslan, M. Candotti, and A. Yarovoy, "Synthesis of multi-beam space-tapered linear arrays with side lobe level minimization in the presence of mutual coupling", in *Proc 13th EuCAP*, Krakow, Poland, Apr. 2019.
- [24] A. F. Morabito, A. R. Lagana, G. Sorbello, and T. Isernia, "Mask constrained power synthesis of maximally sparse linear arrays through a compressive-sensing-driven strategy," *J. Electromagn. Waves Appl.*, vol. 29, no. 10, pp. 1384-1396, 2015.
- [25] A. F. Morabito and P. Rocca, "Reducing the number of elements in phase-only reconfigurable arrays generating sum and difference patterns," *IEEE Antennas Wireless Propag. Lett.*, vol. 14, pp. 1338-1341, 2015.
- [26] C. Yan, P. Yang, and S. Y. Huang, "Synthesis of planar sparse arrays with minimum spacing constraint," *IEEE Antennas Wireless Propag. Lett.*, vol. 17, pp. 1095-1098, Jun. 2018.
- [27] X. Li, B. Duan, J. Zhou, L. Song, and Y. Zhang, "Planar array synthesis for optimal microwave power transmission with multiple constraints," *IEEE Antennas Wireless Propag. Lett.*, vol. 16, pp. 70-73, Apr. 2016.
- [28] M. D'Urso, G. Prisco, and R. M. Tumolo, "Maximally sparse, steerable, and nonsuperdirective array antennas via convex optimizations," *IEEE Trans. Antennas Propag.*, vol. 64, no. 9, pp. 3840-3849, Sep. 2016.
- [29] Y. Aslan, J. Puskely, A. Roederer, and A. Yarovoy, "Synthesis of multiple beam linear arrays with uniform amplitudes," in *Proc. 12th EuCAP*, London, UK, Apr. 2018.
- [30] P. You, Y. Liu, S. Chen, K.-D. Xu, W. Li, and Q. H. Liu, "Synthesis of unequally spaced linear antenna arrays with minimum element spacing constraint by alternating convex optimization," *IEEE Antennas Wireless Propag. Lett.*, vol. 16, pp. 3126-3130, 2017.
- [31] H. Lebreit and S. Boyd, "Antenna array pattern synthesis via convex optimization," *IEEE Trans. Signal Process.*, vol. 45, no. 3, pp. 526-532, Mar. 1997.
- [32] *Ansoft High Frequency Structure Simulator (HFSS), Ver. 15*, Ansoft Corp., Pittsburgh, PA, USA, 2013.